Distinct Proximal and Distal Corticospinal Signals Embed Limb Dynamics Through the Modulation of Stiffness

R. L. Hardesty[1], P. H. Ellaway[2], and V. Gritsenko[1]

[1] Department of Human Performance, Department of Neuroscience, Rockefeller Neuroscience Center, West Virginia University, Morgantown, WV, USA

[2] Department of Medicine, Imperial College London, London, UK

Abstract

The complexities of the human musculoskeletal system and its interactions with the environment creates a difficult challenge for the neural control of movement. The consensus is that the nervous system solves this challenge by embedding the dynamical properties of the body and the environment. However, the modality of control signals and how they are generated appropriately for the task demands are a matter of active debate. We used transcranial magnetic stimulation over the primary motor cortex to show that the excitability of the corticospinal tract is modulated to compensate for limb dynamics during reaching tasks in humans. Surprisingly, few profiles of corticospinal modulation in some muscles and conditions reflected Newtonian parameters of movement, such as kinematics or active torques. Instead, the overall corticospinal excitability was differentially modulated in proximal and distal muscles, which corresponded to different stiffness at proximal and distal joints. This suggests that the descending corticospinal signal determines the proximal and distal impedance of the arm for independent functional control of reaching and grasping.

Significance Statement

The nervous system integrates both the physical properties of the human body and the environment to create a rich repertoire of actions. How these calculations are happening remains poorly understood. Neural activity is known to be correlated with different variables from the Newtonian equations of motion that describe forces acting on the body. In contrast, our data show that the overall activity of the descending neural signals is less related to the individual Newtonian variables and more related to limb impedance. We show that the physical properties of the arm are controlled by two distinct proximal and distal descending neural signals modulating components of limb stiffness. This identifies distinct neural control mechanisms for the transport and manipulation actions of reach.

Introduction

Movement and Limb Dynamics

Neuromechanics is a new field of neuroscience that combines biomechanics with motor control (Nishikawa et al., 2007; Prochazka and Yakovenko, 2007; Ting et al., 2015; Hardesty et al., 2019). At its base is the understanding that the central nervous system (CNS) imbeds the physical laws of nature, which determine how forces exerted by the muscles and tendons cause motion of body segments in presence of anatomical constraints, inertia of the body, and external forces, for example gravity or contact forces. Newtonian equations of motion describe how all forces acting on a body cause its movement. For the human arm, which consists of multiple segments linked by joints, these equations get rather complex and contain multiple terms. The complexity arises from the propagation of forces along the kinematic chain of the multisegmented body, so that forces applied at one joint cause motion of other joints. This is true for both active self-generated forces due to muscle contractions and for passive external forces due to gravity or object interactions. The overall effect of both active and passive forces can either be assistive and cause motion in the desired direction, or resistive and oppose the desired motion. Therefore, for efficient motor control, the motor commands generated by the CNS must be appropriate to overcome the resistive forces and not interfere with the assistive forces. We have shown that the motor commands generated by the primary motor cortex can compensate for self-generated interaction forces during planar reaching movements with unchanging gravity load on the arm (Gritsenko et al., 2011). However, during natural reaching movements, the gravity force acting on the joints is changing due to the rotation of arm segments relative to the gravity vector. In the current study, we asked the question of whether the control signals generated by the primary motor cortex account for both the active and passive gravitational forces during unconstrained reaching to virtual targets. Our results show that both the active and passive dynamics is imbedded in the signals generated by the primary motor cortex with the purpose of controlling limb impedance.

The emergent complexity of a multivariate dynamical system, such as the neuromuscular system, should be approximated at the appropriate scales that allow for the phenomenological description of the emergent behavior (Anderson, 1972). Occam's razor principle dictates that the scale must be the simplest possible model that captures the behavior of interest. The behavioral manifold of the human arm is commonly described by the dynamical model of the inertial segments linked by viscous joints with biological constraints (Hollerbach and Flash, 1982; Flash and Hogan, 1985; Shadmehr and Mussa Ivaldi, 1994; Gribble and Ostry, 1999; Gritsenko et al., 2009). Similarly, the behavioral manifolds of the different hierarchal levels of the CNS can be represented with models capturing network dynamics. The motoneuron pool dynamics can be described by models of simple integrators (Fuglevand et al., 1993). The motor cortical network dynamics can be described with simplified models that capture low dimensional space of neural manifolds that represent dynamical states or modes of operations (Gallego et al., 2017), including damped oscillators (Churchland et al., 2012). Here we used a combined computational and experimental approach to describe the behavioral manifold of human motor control system with neuromechanical models. We applied single-pulse transcranial magnetic stimulation (TMS) to the human primary motor cortex to perturb the inputs into the neuromechanical dynamical system and observe the gains of the control signals (Gritsenko et al., 2011). This approach is commonly used in control systems engineering; here we have applied it for the first time to study the control systems of the human CNS. Pilot results have been presented in abstract form (Hardesty et al., 2016).

Methods

Subjects

All procedures in this study were approved by the West Virginia University Institutional Review Board (Protocol #1309092800). Potential participants were screened to exclude individuals with any musculoskeletal pathologies or injuries, prior history of seizures or fainting, tinnitus, or psychoactive medications. Informed consent was obtained prior to the start of experiments. We recruited 10 healthy human participants (6 male, 4 female, 24.3 ± 1.8 years old, 76.3 ± 14.5 kg). All participants reported to be right-hand dominant.

Electromyography

Muscle activity and responses to TMS were recorded in twelve upper limb muscles using Trigno (Delsys Inc.), a wireless surface electromyography (EMG) system. The recorded muscles included four muscles spanning the shoulder, i.e. pectoralis (Pec), anterior deltoid (AD), posterior deltoid (PD), and teres major (TM), three muscles spanning both shoulder and elbow, i.e. the long heads of triceps brachii (TriLo) and biceps brachii (BicL) and the short head of biceps brachii (BicS), two muscles spanning only the elbow, i.e. the lateral head of triceps (TriLa) and brachioradialis (BR), and three muscles spanning the wrist, i.e. flexor carpi radialis (FCR), flexor carpi ulnaris (FCU), and extensor carpi radialis (ECR). Muscles were identified based on anatomical landmarks and palpation during contraction; EMG sensors were placed on muscle bellies oriented longitudinally along the muscle fibers (sensor contacts traversed the muscle fibers). EMG signals were sampled at 2 kHz with a gain of 1000.

Kinematics and dynamics

Concurrently with EMG, reaching movements were recorded with motion capture using the Impulse system (PhaseSpace). Nine LED markers were placed on bony landmarks of the arm and trunk using the best practice guidelines (Robertson et al., 2013). Marker coordinates were sampled at 480 Hz using Recap software (PhaseSpace). During the experiment, arm postures and reaching goals were defined using color-coded spherical targets 8 cm in diameter in virtual reality (VR) environment created using Vizard software (WorldViz) and Oculus headset (Fig. 1A). To minimize the inter-subject differences in motion, the locations of all targets were calculated mathematically based on subject's segment lengths and desired shoulder and elbow joint angles (wrist angle was kept at zero). The VR system displayed these targets relative to each subject's shoulder at distances scaled to the subject's arm length, which resulted in finely controlled motions. The targets defined a set of "designer" movements with diverse dynamical contexts where the movement was either largely passive (Control task), or interaction torques were resistive with increasing gravitational load (Resistive task), or interaction torques were assistive with decreasing gravitational load (Assistive task) as described in detail in Hardesty et al. (2019). The dynamical contexts of these movements and their selection was driven by inverse simulations performed with a dynamical model of the arm (Fig. 1B). Movements from different starting points with shoulder and elbow joint excursions that enabled segment rotations in the same direction with resistive interaction torques or in the opposite direction with assistive interaction torques were simulated in presence of gravity. The movements that varied the dynamical conditions the most while maintaining similar endpoint trajectory length were selected. These selected movements were associated with the specific starting and ending shoulder and elbow angles, which were then used to calculate the target locations displayed in VR for each subject using trigonometry.

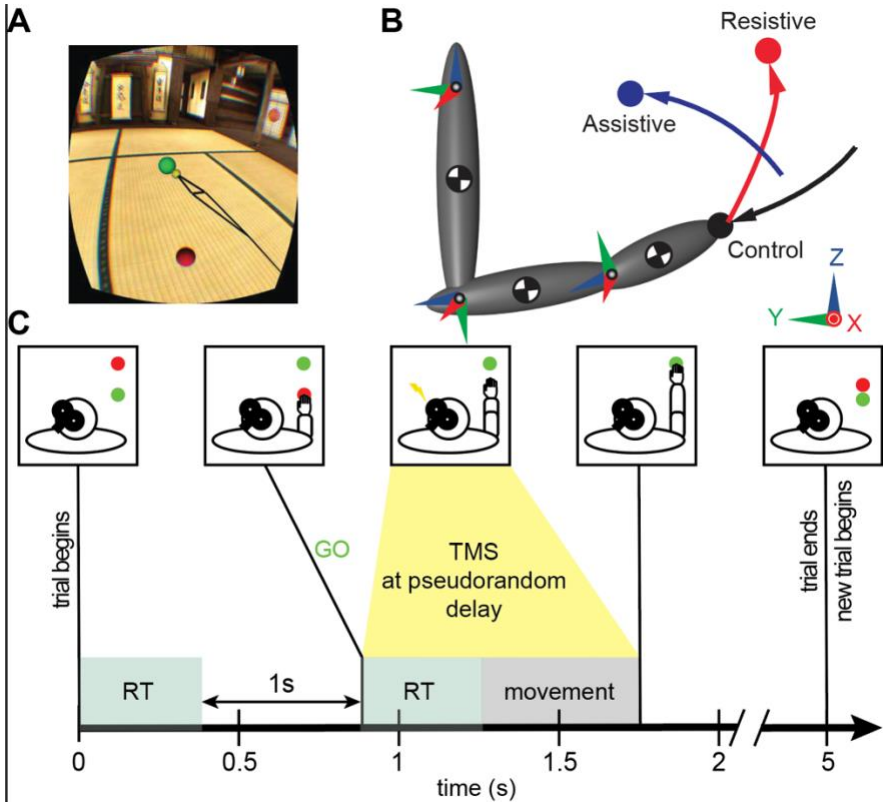

Figure 1. Experimental paradigm. *A. Participant's view of the tasks in virtual reality. Black lines connect LED markers and show the arm position and orientation in VR relative to targets. The yellow sphere represents the fingertip LED on the index finger, which the participants were instructed to move to the center of the green target. B. Schematic of the dynamic model used to calculate joint angles and torques from motion capture and representative endpoint trajectories from the three tasks. C. Approximate timeline of events during a single trial of a movement task. RT stands for reaction time; GO represents the color cue to start movement. When the trial begins, the green target indicates the start location, the red target indicates the stop location. Once the GO event occurs, the colors switch.*

During experiments, motion capture was used to visualize the participant's arm in VR. The marker locations were streamed to VR and used to represent the three main segments of the arm (hand, forearm, and upper arm) as a stick figure (Fig. 1A). Motion capture, EMG, and virtual events were synchronized using custom hardware as described in Talkington et al. (2015).

After experiments, motion capture was used to calculate active muscle torques at shoulder, elbow, and wrist joints using the same dynamical model used for the selection of tasks (Fig. 1B) as described in detail in Olesh et al. (2017). Briefly, the model was customized to each participant's morphology by scaling model segment lengths to match the participant's arm length and scaling model mass to participant's weight using Winter's morphology (Winter, 2009). Inverse simulations were then ran using the motion capture data to obtain active torques produced by the muscles to make the movements in presence of gravity and limb inertia. The axes of joint rotations defined by segment coordinate systems are illustrated in Fig. 1B. Analysis was done on the angles and torques around the X axes, i.e. flexion/extension degrees of freedom at all three joints, because motion was primarily in the sagittal plane and out-of-plane torques were negligible. The active muscle torques at each joint were then subdivided into gravitational and dynamic components to examine the different roles CNS may play in the compensation for gravity and movement production (Olesh et al., 2017).

Transcranial magnetic stimulation

We assessed corticospinal excitability for each participant using single-pulse TMS delivered by the Super Rapid stimulator with a figure-of-eight coil (Magstim). The coil was placed tangentially to the scalp, oriented at a 45° angle to the midline with the handle pointing posteriorly and laterally (Fig. 1C). The coil location over the scalp and its orientation was maintained using the Brainsight neuronavigation system (Rogue Research). The location of stimulation was selected using the hot-spot method (Traversa et al., 1997; Ellaway et al., 1998), during which the coil was moved over the estimated location of the primary motor cortex until a location was found where at least 50 μV motor evoked potential (MEP) in BicS was evoked with the lowest amplitude of stimulation. Resting motor threshold was then determined at this location by varying the stimulation intensity until a MEP > 50 μV was evoked 50% of the time in BicS. BicS was used to define the threshold in order to ensure that MEPs in proximal muscles will be evoked during movement (Gritsenko et al., 2011). Stimulations were performed at intervals greater than 5 s (0.2 Hz) to avoid any long-term changes in corticospinal excitability (Chen et al., 1997). Trials with TMS were grouped into two sessions on the same day.

Session 1: static posture

To evaluate the "background" state of the motor system for maintaining posture without goal-directed motion, we measured MEPs when the participants held their arm at postures corresponding to locations of virtual targets used to direct motion tasks (Fig. 1B). Participants held their arm in one of five static postures, as the starting position for the Resistive task was the same as the ending position for the Control task. Participants were asked to reach to the displayed VR target that corresponded to one of the postures and hold their arm in that posture while we applied 12 TMS pulses at < 0.2 Hz at 90% of resting motor threshold. After that they were instructed to reach to the next target and hold the next posture, etc.

Session 2: movement trials

Once stimulation location and intensity were determined, we asked participants to complete three reaching tasks in the sagittal plane with their dominant (right) arm. Participants were asked to reach only with their arm (no trunk motion), keep their elbow close to their trunk, and keep the wrist straight and palm down. The three tasks were presented to the participants in the same pseudorandom order. Each trial started with the appearance of start and stop targets, the former of green color and the latter of red color (Fig. 1C). The colors and target locations did not change until the participants placed their index finger indicated with a yellow sphere into the start target. One second after this the stop target changed color from red to green, directing the participants to begin the movement (Fig. 1C). Each movement was repeated for 138 repetitions (total of 414 trials).

Movement trials were designed to probe the corticospinal excitability at multiple time points directly preceding and during movement. These trials were divided into stimulation trials (126 per movement, 378 total) with non-stimulation control trials (12 per movement, 36 total) interspersed randomly. TMS was performed at 90% of the resting motor threshold. In one half of trials (189 of 378), the TMS was triggered at a random delay of 0 – 550 ms after the participant touched the start target. In the other half of trials, the TMS pulses were triggered when the participant left the start target after a random delay of 0 – 550 ms. The different triggering events ensured a distribution of TMS pulses prior to and during movement. The timing of each TMS pulse was recorded relative to both EMG and kinematics for post-hoc synchronization and analysis.

MEP Quantification and Normalization

We assessed corticospinal excitability by quantifying MEP magnitudes and normalizing them to background muscle activity. Quantification was performed by integrating a 40ms period of rectified EMG recordings at times beginning 10ms after each stimulation (Fig. 2A). The selected

window ensured that the integrated time period encompassed the entire MEP. Quantifying the changes in corticospinal excitability during active movement is confounded by the changing motoneuronal excitability on which corticospinal projections terminate. Previous studies have found that MEP magnitude scales linearly with muscle activity (Darling et al., 2006). Therefore, we used the ratio of MEP magnitude to background EMG activity recorded during our static trials for each muscle to calculate an expected or 'predicted' MEP amplitude based on the background activity. These ratios provided a simple relationship of MEP magnitudes during different levels of isometric contraction. To calculate a predicted MEP magnitude, we multiplied the ratios (*b*) by the average background EMG activity at the same time periods, which were recorded during non-stimulation control trials (Fig. 2B) as follows:

$$MEP_{Pred} = b \times EMG \qquad (1)$$

Then we compared our predicted MEPs to those recorded during movement trials and defined two measures of MEP size. The first measure was MEP amplitude, which was defined as the ratio between the MEP magnitude and the static MEP magnitude in the starting posture of the corresponding task. This measure defined the modulation of corticospinal excitability relative to the static posture that corresponded to the starting position for each movement. The second measure was MEP gain defined as follows:

$$Gain = \frac{MEP_{Dyn}}{MEP_{Pred}} \qquad (2)$$

where MEP_{Dyn} is the MEP magnitude recorded at a certain phase of movement and MEP_{Pred} is predicted magnitude using eq. (1) based on the background EMG at the corresponding phase of movement. This measure defined the modulation of corticospinal excitability that was independent from EMG and enabled the assessment of corticospinal modulation upstream of motoneurons.

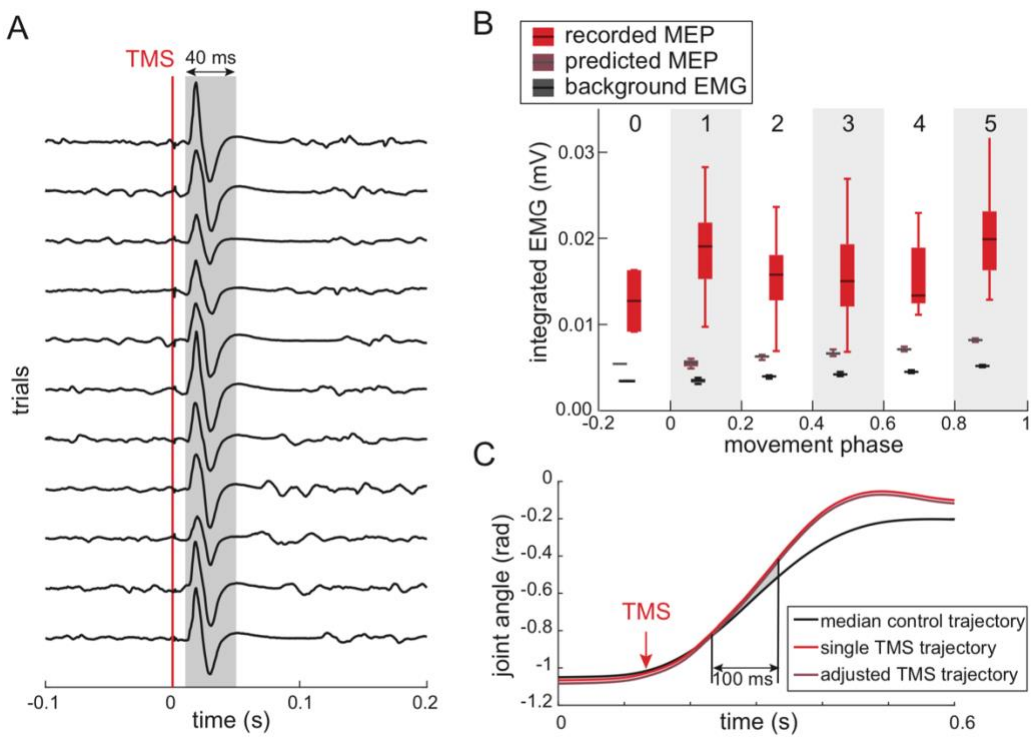

Figure 2. Quantifying MEPs. *A. Multiple trials of MEP responses and the integration window which was used to quantify MEP amplitude from rectified signals (not shown). B. Magnitudes of EMG, predicted MEPs,*

and recorded MEPs binned together relative to their time during a movement, where 0 denotes the kinematic onset of movement and 1 denotes the kinematic offset. C. The illustration of the quantification of TMS responses in angular kinematics.

Quantification of Kinematic Perturbations

In addition to quantifying MEP responses, we wanted to quantify the kinematic effect of cortical stimulation. TMS generates transient "twitches" in effected muscles that can result in movement. We integrated a 100ms time window of single-trial joint angle profiles immediately following stimulation. We then calculated the difference between the perturbed kinematics and the median trajectory of non-stimulation control trials (Fig. 2C). Any initial offsets due to inter-trial variability were subtracted prior to integration.

Statistical Analyses

MEPs collected during static trials were linearly regressed to EMG amplitude at a significance criterion of 0.05. TMS responses during movement were grouped into 5 bins each comprised 20% increments of phase duration from onset to offset of movement (Fig. 2B). To accurately estimate MEP amplitudes preceding movement, TMS responses that occurred up to 20% phase duration prior to movement were grouped into a bin 0 (Fig. 2B). This binning procedure amalgamated MEPs occurring at similar times during movement, providing adequate repetitions to estimate mean values. We defined a minimum repetition criterion of 5 MEPs based upon (Lewis et al., 2014). Bins that contained < 5 MEPs were excluded from subsequent analyses. The same binning procedure was repeated for all other signals that are compared to MEPs using the time stamps of TMS responses in phase domain.

The presence of corticospinal modulation relative to static condition was determined using a non-parametric Wilcoxon Rank-Sum test, which compared mean MEP amplitudes and MEP gains to 1 for each bin, task, and muscle across subjects. Significant values are reported in Figures 6 and 7 as dots above bars. The presence of kinematic responses to TMS was determined using t-tests, as these values were normally distributed. Significant values are reported in Figure 8 as dots above bars.

Additionally, single-trial binned MEP and EMG amplitudes were bootstrapped independently for 100 iterations while preserving the structure of the data (Efron and Tibshirani, 1993). This means that single-trial MEPs and corresponding EMG values were sampled with replacement separately for each movement bin, each task, each muscle, and each participant. Each bootstrap was averaged first within each subject and the across subjects to maintain equal contribution of individuals to the overall distribution. The Wilcoxon sign rank test was applied to these bootstrapped values and the results were similar to that obtained from the original experimental data without bootstrapping. Therefore, statistics on bootstrapped data is not included in the manuscript.

To test a hypothesis that the TMS gain profiles are linearly related to individual kinematic and dynamic variables, we performed a regression analysis.

Results

Corticospinal Excitability During Posture Maintenance

Maintaining limb posture against gravity requires active neural control to compensate for the complex anatomy of our bodies and the imprecise and noisy biological control signal (Harris and Wolpert, 1998). In the current study, we found evidence supporting the contribution of the corticospinal tract to posture maintenance. At stimulation amplitudes below resting motor threshold, we observed MEPs in most muscles, even in those muscles that did not show changes

in EMG amplitudes associated with holding the arm against gravity (Fig. 3A and B). This indicates that when the arm is held in a certain posture the corticospinal excitability increases so that it contributes more to the motoneuronal excitability compared to when the arm is relaxed.

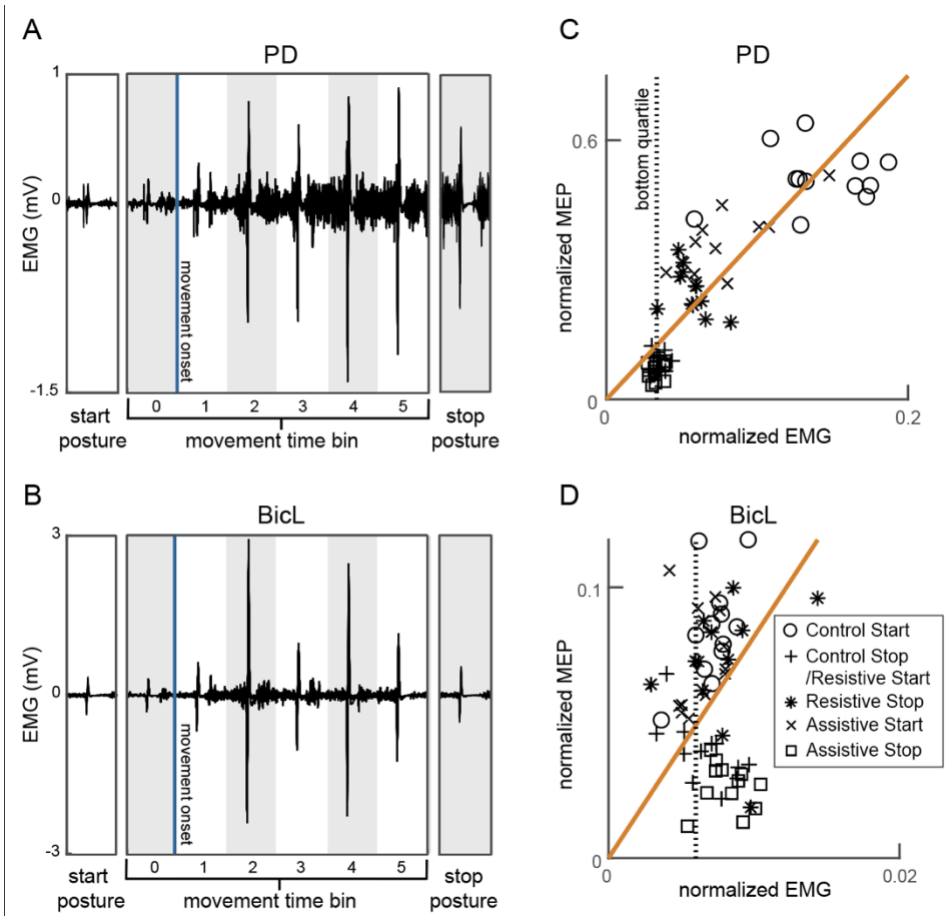

Figure 3. Postural Corticospinal Excitability. *A, B. Superimposed MEP/EMG repetitions for two muscles are shown from one subject, where A shows a muscle with a significant linear fit between MEP and EMG amplitudes and B shows a muscle with a non-significant fit. C. An example of the clear linear relationship between MEP and EMG amplitudes observed in two-thirds of the recorded muscles. The bottom quartile of EMG values is shown by the dashed line. D. An example of a muscle which does not demonstrate a significant linear fit, presumably due to the smaller range of EMG amplitudes.*

We found that static MEP amplitudes scaled linearly with EMG amplitude for most of the muscles across all static postures. The linear regression was significant with $p < 0.05$ in 80 out of 120 cases across 12 muscles in 10 subjects (Table 1, Fig. 3C). In the 40 cases with insignificant linear regressions (Fig. 3D), muscles were recruited to a lesser extent across different postures. The difference in median EMG maxima between muscles which had “good” and “poor” fits was 0.22 or 21.70% (one-sided, Wilcoxon Rank-Sum test $p = 0.018$). The “good” regressions provided us a confident estimate of the MEP gain required for posture maintenance in a given muscle (see Methods, eq. (1)). We also assumed that the “poor” regressions provided ratios between static MEP amplitudes and EMG that can be used to approximate MEP gain for a given posture. We tested this assumption by calculating ratios between the bottom quartile of EMG values and their corresponding MEPs for the 80 cases with significant linear regressions and comparing them to the slopes obtained over the full range. We found no difference between the bottom-quartile ratios

and slopes (Wilcoxon Rank-Sum test $p > 0.05$) and a small normalized root-mean-squared-error of 0.0205 (normalized to the range of the data) between the corresponding ratios and slopes. This supports the validity of using the ratios between static MEPs and EMG to estimate the MEP gain for posture in muscles that do not actively participate in holding the arm against gravity.

Table 1: The distribution of MEP vs EMG slopes in static posture task.

Muscle	Median slope	25th %	75th %
Pec	1.47	1.24	2.22
AD	1.90	0.98	3.26
PD	2.08	1.18	3.75
TM	1.68	1.18	2.14
TriLo	2.30	1.41	5.12
TriLa	3.32	1.58	5.80
BicL	4.77	1.68	7.27
BicS	4.29	1.85	6.38
BR	6.52	5.28	11.06
FCR	4.83	2.57	8.26
FCU	5.43	3.31	9.60
ECR	5.32	2.97	6.30

The linear relationship we found between MEPs and EMG is consistent with previous work by Darling et al. (2006). Alternatively, Tazoe et al. (2007) found that increases in MEP amplitude become saturated at higher intensities of muscle activity (> 60% MVC). However, in our study participants were asked to complete gross reaching tasks with no additional load than the weight of the arm, which made it unlikely that any movement exceeded this linear range. Therefore, we used the ratios between static MEPs and EMG to normalize the MEPs during movement (see Methods, eq. (2)).

The Role of Limb Dynamics During Reaching

The locations of virtual targets used in this study were selected using a biomechanical model of the arm so that movement was accompanied by gravitational and other inertial forces in specific directions. These forces created unique challenges for the control of limb dynamics by the CNS and defined our Control, Assistive, and Resistive tasks (see Methods: Movement Tasks). The virtual targets were very effective in evoking the desired behavior and standardizing the movement kinematics and dynamics across all participants. In the Control and Assistive tasks, the shoulder and elbow rotated in opposite directions (Fig. 4A, black and blue). This motion is assisted by interaction torques that amplify the active muscle torques (Fig. 4D, black and blue). In our Assistive task, gravity load decreased during movement at the shoulder and elbow joints. (Fig. 4C, blue) This relationship can be observed from the lower muscle torques that were required to hold the arm at the end of movement compared to the torques at the beginning of movement (Fig. 4B blue). In contrast, in the Resistive task the interaction torques between the shoulder and elbow counteract the desired movement (Fig. 4D, red). This effect is shown in Figure 4 A and B

(red) as gravity was increasing at the shoulder and decreasing at the elbow. Interestingly, the overall effect of gravity and limb dynamics in both the Assistive and Resistive tasks were similar at the elbow and wrist despite the differences seen at the shoulder. This relationship can be seen in the similar torque profiles in Fig. 4B (blue and red). Both required peak muscle-torque changes in the same direction to decelerate the forearm and hand in the second phase of movement (Fig. 4C, blue and red vs. black). However, at the shoulder, the dynamic conditions in all three tasks were distinct, where the Resistive and Control tasks had opposite profiles and the Assistive task had a constant extension torque (Fig. 4C first column).

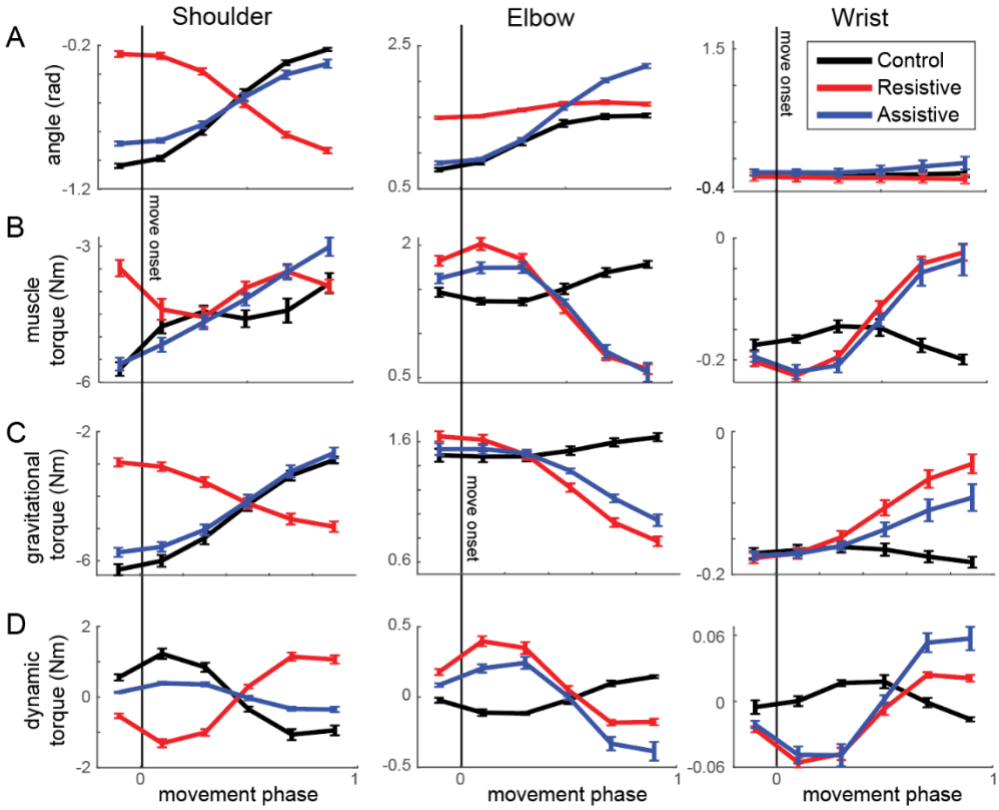

Figure 4. Movement Kinematics & Dynamics. *A. Participant joint angles calculated from motion-capture recorded kinematics. B. Muscle torques calculated using an inverse dynamics model. C. Rotatum calculated based on the differentiation of the muscle torque timeseries data and then binned. Lines denote mean values across subjects and error bars denote standard error of the mean.*

The Compensation for Limb Dynamics by Muscle Contractions

The distinct dynamic conditions of each task were controlled system with distinct patterns of muscle contractions. The pattern of binned EMG closely paralleled the previously reported temporal profiles of muscle activity in these tasks (Hardesty et al., 2019). The pattern indicated task-dependent co-activation of agonists and antagonists. In the Resistive task, muscles that span the shoulder were co-activated more toward the end of movement (Fig. 6 red). The level of co-contraction of the shoulder muscles increased together with the increasing shoulder flexion angle and gravity-related muscle torque at the shoulder. The BicL, BR, and ECR also co-activated with a burst in the beginning of movement (Fig. 6 red) that coincided with the acceleratory peaks in shoulder flexion, elbow flexion, and wrist extension muscle torques (Fig. 5B). In contrast, in the Assistive task most muscles spanning the elbow and wrist (TriLo, TriLa, BicL, BicS, BR, FCR,

FCU, and ECR) coactivated throughout the movement (Fig. 6 blue). This co-contraction was accompanied with decreasing gravity-related muscle torques at all joints (Fig. 5). These results indicate that the CNS controls limb dynamics by co-activating agonistic and antagonistic muscles that span multiple joints.

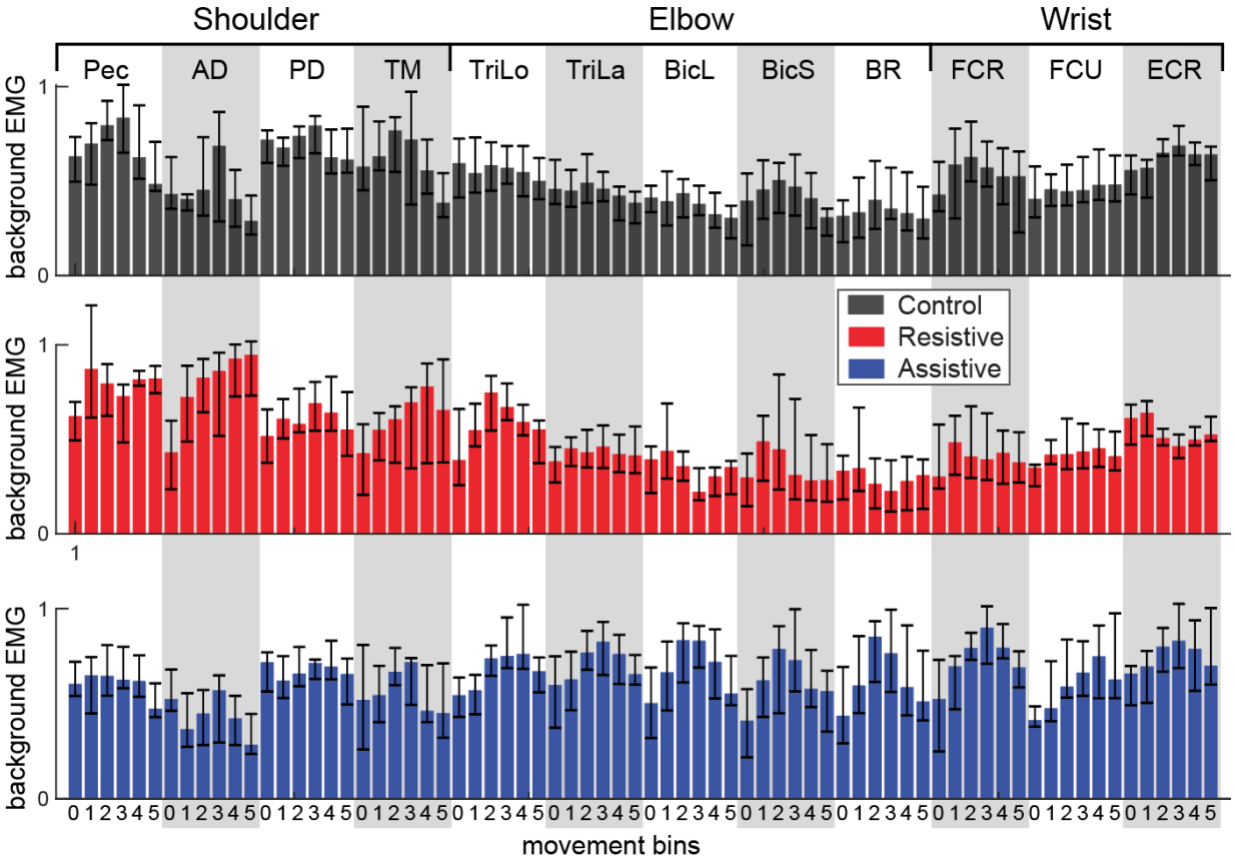

Figure 5. Muscle Activity During Movement. *Muscle activity recorded with EMG displays distinct profiles for different dynamic tasks. Bars denote mean integrated values and error bars show standard error. Values are normalized to maximum across all movements.*

The Compensation for Limb dynamics by Changes in Corticospinal Excitability

The task-dependent, multi-muscle control strategy of the CNS indicated by EMG profiles was further observed in the modulation of corticospinal excitability during movement. MEP amplitudes changed during different phases of movement and these changes were distinct depending upon the task, as shown in Fig. 6. Overall the Control task, which is the most passive movement due to gravity, showed the fewest instances of MEP facilitation (1st time bin in BR) and inhibition in the flexors of the shoulder. The Resistive task, which required shoulder flexion against gravity, demonstrated large facilitation of MEPs in three of four muscles spanning the shoulder (AD, PD, TM) and the long head of the triceps (TriLo). Finally, the Assistive task, which shared similar limb dynamics to the Control task, similarly showed inhibition of MEPs in flexors of the shoulder as well as some moderate facilitation in the flexors of the elbow and wrist. As we expected, based upon our results in Task 1, MEP facilitation seemed to roughly correlate to muscle activity, particularly for muscles spanning the shoulder. For example, the Resistive task showed large increases in MEP amplitudes in the anterior deltoid that seemed to increase as the

movement progressed while MEPs in the Control and Assistive task appeared to be suppressed. We, therefore, calculated the MEP gain, as defined in eq. (2), to assess changes in corticospinal excitability independent of muscle activity as seen in Fig. 8.

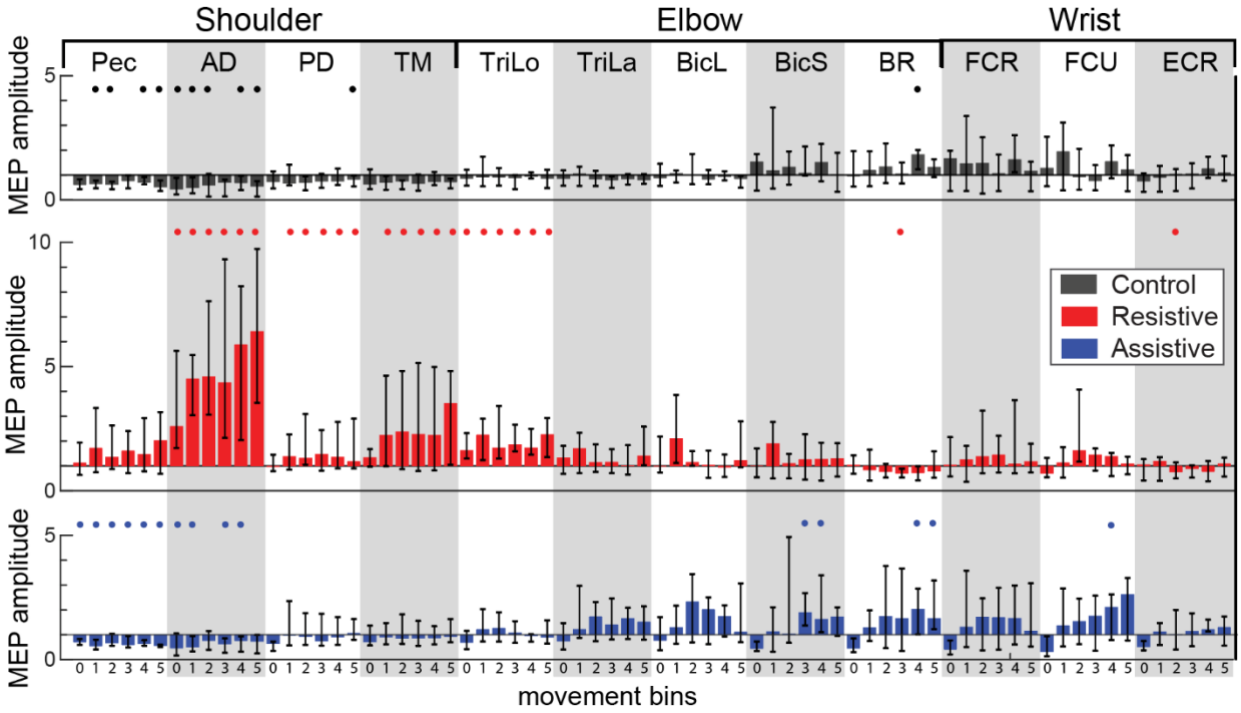

Figure 6: The modulation of corticospinal excitability. *MEP amplitudes during movement show distinct temporal profiles between different reaching tasks. The median change of MEP amplitudes across subjects for control, resistive, and assistive tasks are shown in black, red, and blue respectively and error bars denote interquartile range. MEPs during movement were normalized to the amplitude recorded at the static posture at the start target for each movement. Dots indicate statistical difference from 1 (P<0.05, Wilcoxon Rank Sum).*

We found that MEP gain was also temporally modulated in a task-specific manner. Prior to motion start, both the MEP amplitude and MEP gain were lower than during movement in most muscles and most tasks (Fig. 6 & 7, bin 0). This is consistent with inhibited corticospinal excitability during the preparatory phase prior to movement observed in humans with H-reflex modulation (Hannah et al., 2018). During movement, the MEP amplitudes in muscles spanning the shoulder (Pec, AD, PD, TM) were determined primarily my muscle activity. However, this was not the case for muscles spanning the elbow and wrist. In particular, flexors of the elbow and all muscles of the wrist showed gain values significantly less than 1 ($p < 0.05$ Wilcoxon Rank Sum), this means that MEP amplitudes were smaller than expected based on a scalar proportion to the background muscle activity (Fig. 7). The TMS gain of distal muscles (BicL, BicS, BR, FCR, FCU and ECR) was significantly lower than the TMS gain of proximal muscles (Pec, AD, PD, TM, TrilLo, TriLa) with the mean difference between distal minus proximal TMS gain of -0.30 ± 0.60 across all tasks and muscle groups (one-tailed t-test $p < 0.01$). One potential explanation for TMS gains < 1 could be that the corticospinal pathways are maximally activated by TMS and MEP size saturates. This predicts that the largest MEPs will occur riding on top of the largest background EMG (or that MEPs have constant amplitude regardless of background EMG), and that the largest MEPs will be suppressed the most, i.e. have the most negative MEP gain. However, this is obviously not the case in BicS, BR, and FCU. In these muscles, the largest MEPs occur at the end of the Assistive task (Fig. 6 blue), but the MEP gain is most reduced in the Resistive task and in the first

half of the Assistive task (Fig. 7 blue). Additionally, MEP gain does not explicitly follow the same temporal profile as muscle activity. For example, the largest EMG amplitude in elbow flexors (BicL, BicS, and BR) occurs during the middle of the Assistive task (Fig. 5 blue, bins 2, 3). However, the MEP gain is the lowest prior to and immediately after movement onset (Fig. 7 blue, bins 0, 1) and increase in a linear manner throughout the movement. Therefore, while we cannot rule out that the MEPs may saturate in AD and ECR, we can rule out the saturation for Pec, PD, TM, TriLo, TriLa, BicL, BicS, BR, FCR, and FCU. Overall, we show that neither MEP amplitude nor MEP gain follow the profile of muscle activity in muscles spanning the elbow and wrist, which suggests that motoneuronal excitability that underlies EMG is being driven by some input other than the corticospinal tract.

Surprisingly, we observed a proximal-distal scaling of corticospinal excitability with decreasing MEP gain for more distal muscles across all three tasks. The data defines two control groups, a proximal group of muscles consisting of Pec, AD, PD, TM, TriLo, and TriLa, and a distal group of muscles consisting of BicL, BicS, BR, FCR, FCU, and ECR (Fig. 7, the number of significant bins). The corticospinal input to the proximal group was similar to that expected from postural set and EMG changes, while the corticospinal input to the distal group was lower than expected.

We also observed that the temporal modulation of MEP gain did not correspond linearly with the temporal modulation of most kinematic and dynamic signals. The distribution of regressions between MEP gains in each muscle and joint angles had the median of 0.24 and 0.07 – 0.52 interquartile interval (25th – 75th percentile). The distribution of regressions between MEP gain and muscle torques had the median of 0.18 and 0.06 – 0.43 interquartile interval. The distribution of regressions between MEP gain and gravitational torques had the median of 0.21 and 0.06 – 0.46 interquartile interval. The distribution of regressions between MEP gain and

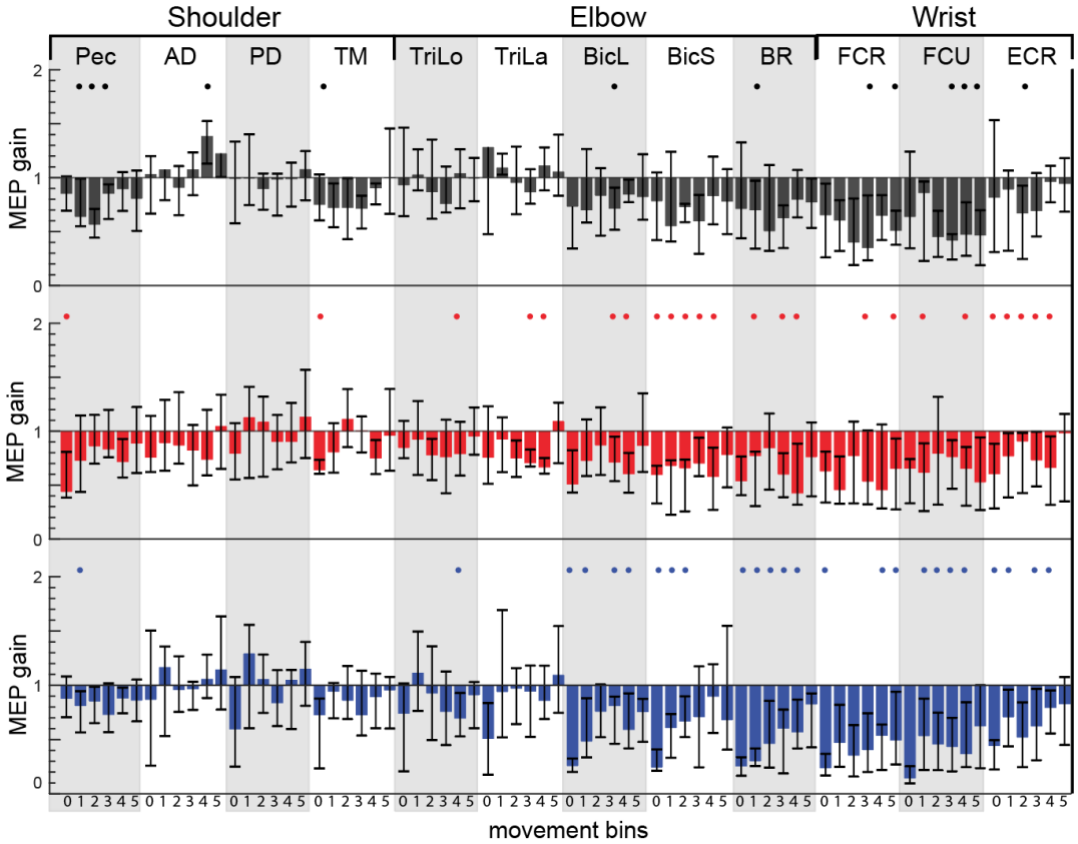

Figure 7: The modulation of MEP Gain. *MEP gain during movement shows distinct temporal profiles independently of muscle activity. The median change of MEP gain across subjects for control, resistive, and assistive tasks are shown in black, red, and blue respectively and error bars denote interquartile range. MEPs during movement were normalized to the amplitude predicted from EMG at corresponding movement bins in Fig. 5 scaled with the static ratio (see Methods). Dots indicate statistical difference from 1 (P<0.05, Wilcoxon Rank Sum).*

dynamic torques had the median of 0.18 and 0.05 – 0.40 interquartile interval. Thus, some linear relationships between the profiles of corticospinal excitability and some kinematic or dynamic parameters existed, but there was no overall pattern that would identify a single modality of the control signal. Altogether, our findings suggest that the corticospinal tract may both directly shape muscle activity patterns, such as those of shoulder muscles, and indirectly contribute to the control of some other physiological variables on a per muscle per task basis depending upon the dynamic demands of the movement.

Motor Responses Evoked by TMS

TMS caused MEPs in all recorded muscles, which in turn produced brief responses in angular trajectories during movement (Fig. 8). The kinematic responses at the shoulder were the smallest and, when significantly different from noise, in the direction of motion (Fig. 8, first column). The direction of shoulder motion switched from extension in Control and Assistive tasks to flexion in Resistive task (Fig. 4A). This pattern of responses agrees well with the modulation of the corticospinal excitability observed in muscles spanning the shoulder, which was proportional to the muscle activity patterns causing the motion (Fig. 6 & 7). The small amplitudes of kinematic responses are likely due to extensive co-activation of shoulder muscles leading to increased joint stiffness during movement compared to posture maintenance. The kinematic responses at both elbow and wrist were toward flexion in all tasks (Fig. 8). This is despite different kinematic and dynamic requirements of these joints in each task (Fig. 4). This pattern of kinematic responses corresponds to the motion caused by contraction of muscles with reduced MEP gain during

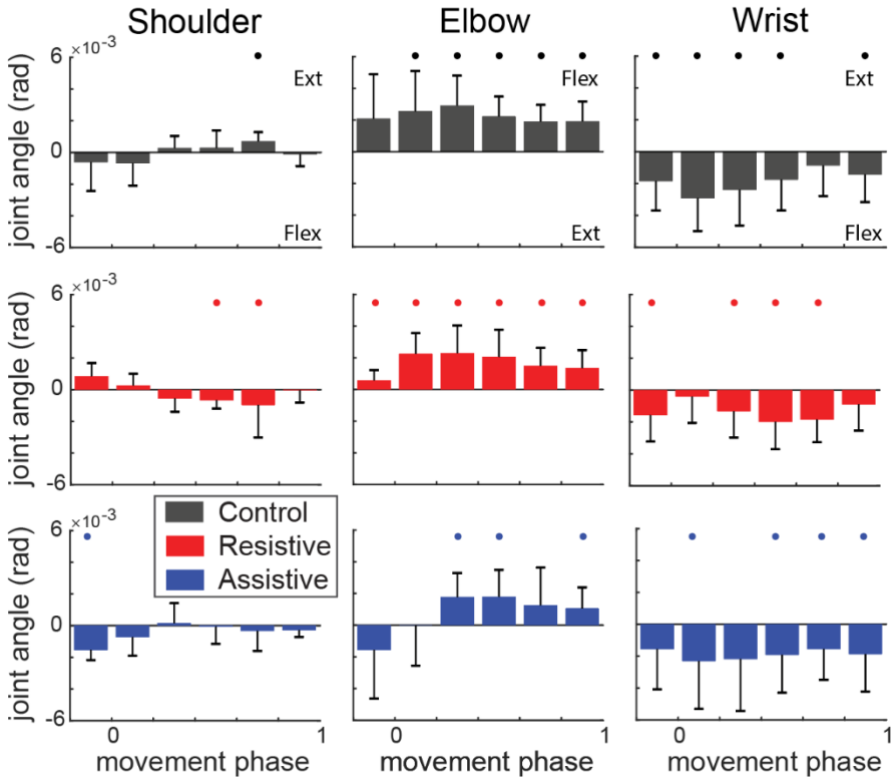

Figure 8. Motor responses to TMS that resulted from MEPs*. Kinematic perturbations due to TMS were compared to non-stimulation control movements. Joint angles were quantified with a 100ms integration window at a delay of 100ms after the time of stimulation in both single MEP trials and the mean non-stimulation control movements. Bars denote the mean difference between MEP trials and control trials and error bars show standard deviation across subjects. Ext denotes extension direction of rotation; Flex denotes flexion direction of rotation for corresponding joints.*

movement (BicL, BicS, BR, FCR, and FCU, Fig. 7). The amplitudes of kinematic responses at the elbow and wrist were larger than those at the shoulder (Fig. 8 the number of significant bins). Together with the reduced TMS gain to distal muscles, this suggests reduced elbow and wrist stiffness during movement compared to during posture maintenance.

Discussion

Here we have taken advantage of Newtonian physics to design unconstrained reaching tasks in VR and precisely manipulate the passive forces acting on the human arm. During these tasks, we probed the gain of the corticospinal contribution to the compensation for these forces. We observed active corticospinal control of all recorded muscles, as evidenced by the presence of MEPs in all muscles during stimulation below resting motor threshold. We further found that during movement the corticospinal extricability was modulated independently from motoneuronal excitability with different profiles in individual muscles that varied with each task (Fig. 7). The perturbations of TMS to this modulation resulted in the smallest deviations from the desired trajectory at the shoulder and larger deviations at elbow and wrist, which corresponded to flexor synergy (Fig. 8). This suggests that both the active and passive forces acting on the limb during a stereotypical reaching motion are imbedded in the corticospinal pathway not as individual kinematic or dynamic variables, but rather as a wholistic control signal that modulates limb impedance.

Here we used a novel TMS paradigm to investigate the temporal modulation of corticospinal excitability inspired by our previous work with TMS during planar movements (Gritsenko et al., 2011). We applied TMS over the primary motor cortex at 90% of resting motor threshold with a 45° posterior-anterior coil orientation to preferentially activate pyramidal tract neurons (Kaneko et al., 1996; Nakamura et al., 1996; Di Lazzaro et al., 1998) and generate responses proportional to cortical activity (Baker et al., 1995; Carson et al., 1999; MacKinnon and Rothwell, 2000; Di Lazzaro et al., 2003; Cros et al., 2007). The corticospinal tract and other descending tracts converge on the motoneurons, the final common pathway. Therefore, TMS responses are also modulated by the excitability of those motoneurons (MacKinnon and Rothwell, 2000; Darling et al., 2006; Taylor, 2006; Groppa et al., 2012). Here we too observed that the TMS responses were linearly modulated by the motoneuronal excitability estimated from EMG during static postures (Table 1). We used this linear relationship to calculate TMS gain as a measure of CST excitability independent from the contribution of spinal motoneuron excitability. Amazingly, this simple linear relationship described a lot of changes in MEP sizes during movement as evidenced by multiple MEP amplitude and MEP gain values in different conditions being close to 1 (Fig. 6 & 7). This suggests a minimum intervention principle of the motor control circuits only contributing enough to displace the dynamical system from one static (steady) state to another, consistent with optimal control theories (Hogan, 1984; Todorov and Jordan, 2002). The kinematic responses to TMS further supported this view by demonstrating task-dependent modulation consistent with task dynamics (Fig. 8). This further validates our assumption that the TMS did not simply disrupt the activity of the corticospinal tract, but rather perturbed it in proportion to current activity. Altogether, our data supports the validity of using single-pulse TMS during movement

constrained by virtual reality to study non-invasively the descending corticospinal activity in humans.

Mechanical impedance is defined by the reaction of the musculoskeletal system to perturbations (Mizrahi, 2015); it consists of stiffness and viscosity components. Muscle contractions result in forces that act in either the same or opposite directions around each degree of freedom of the joints they span as determined by muscle anatomy (Gritsenko et al., 2016). These counterbalanced forces define the mechanical stiffness component of impedance based on the spring-like properties of muscles and tendons (Brown and Loeb, 2000; Valero-Cuevas et al., 2015). Previous research has shown that mechanical impedance estimated with co-contraction of antagonistic muscles varied with the stability of the movement (Burdet et al., 2001; Rancourt and Hogan, 2001; Milner, 2002). Here we also observed increased co-contraction in the most unstable movement in the Assistive task (Fig. 5 blue) (Hardesty et al., 2019). Furthermore, we observed modulated corticospinal excitability in all muscles, agonists and antagonists, during both postural and motion tasks (Table 1; Fig. 6 and 7). The temporal profile of this modulation during movement was not correlated with either kinematic or dynamic variables of these movement. Instead, the changes in corticospinal excitability during movement lead to variable joint stiffness across tasks and joints as evidenced by motor responses to TMS (Fig. 8). This argues against the modality of the corticospinal control signals being based on Newtonian variables of motion, i.e. kinematics or moments. Instead, our evidence supports the idea of an impedance control signal that includes at least the stiffness component for proximal and distal parts of the arm. The activity of individual neuronal populations in the primary motor cortex observed to be related to kinematic and dynamic parameters of motion (Evarts, 1968; Georgopoulos et al., 1986; Kalaska et al., 1997; Scott, 2004) may be combined into a more wholistic corticospinal descending signal and shaped by the subcortical structures to result in the impedance control signal observed here. Of note is that the TMS perturbation to motion did not cause oscillations, which suggests that the corticospinal commands ensure that the neuromusculoskeletal system is critically damped. Altogether, these commands can control the endpoint stiffness appropriately to compensate for limb dynamics and external forces as suggested by earlier studies of motor adaptation to dynamical perturbations (Takahashi et al., 2001; Milner and Franklin, 2005; Selen et al., 2009).

Reaching movements are often separated into two distinct actions 1) the transport action that involves large excursions of shoulder and elbow joints to transport and orient the hand and 2) the manipulation action that involves the interaction of the hand with objects. This separation is reflected in the organization of muscle anatomy, where functional changes in muscle lengths are similarly divided into proximal and distal clusters (Gritsenko et al., 2016). This mechanical organization is also reflected in the nervous system. Neural stimulation experiments have shown that cortical muscle representations are also organized somatotopically based on their proximal-to-distal anatomy (Penfield and Rasmussen, 1950; Wassermann et al., 1992). Similarly, distinct white matter tracts demonstrate some preferential contribution for proximally-controlled gross movements versus distally-controlled fine motor skills (Lawrence and Kuypers, 1968). For these reasons, corticospinal excitability has been shown to differentially modulate for proximal and distal muscles depending upon the demands of a particular task, i.e. reaching vs grasping (Schieppati et al., 1996). Here we also observed distinct modulation of corticospinal excitability in proximal and distal muscles, where distal muscles were associated with lower MEP gain during movement compared to proximal muscles (Fig. 7). This is despite all three tasks being gross reaching movements and not requiring the fine manipulation with the hand. Furthermore, we observed differential amplitudes in motor responses to TMS (Fig. 8) indicating different proximal and distal joint stiffnesses. Altogether, this evidence suggests that there may be two distinct proximal and distal controllers of the arm. The proximal controller may be more energetically favorable for

controlling arm impedance (Nguyen and Dingwell, 2012) and driving the transport action (Dounskaia, 2010). The distal controller may be more attuned to the object interaction demands than the biomechanics of the transport action (Downey et al., 2017).

References

Anderson PW (1972) More is different. Sci (New York, NY) 177:393–396 Available at: http://www.sciencemag.org/cgi/doi/10.1126/science.177.4047.393.

Baker SN, Olivier E, Lemon RN (1995) Task-related variation in corticospinal output evoked by transcranial magnetic stimulation in the macaque monkey. J Physiol 488 (Pt 3:795–801 Available at: http://jp.physoc.org/cgi/reprint/488/Pt_3/795.

Brown IE, Loeb GE (2000) A Reductionist Approach to Creating and Using Neuromusculoskeletal Models. In: Biomechanics and Neural Control of Posture and Movement, pp 148–163. New York, NY: Springer New York. Available at: http://link.springer.com/10.1007/978-1-4612-2104-3_10.

Burdet E, Osu R, Franklin DW, Milner TE, Kawato M (2001) The central nervous system stabilizes unstable dynamics by learning optimal impedance. Nature 414:446–449 Available at: http://www.nature.com/nature/journal/v414/n6862/abs/414446a0.html.

Carson RG, Riek S, Bawa P (1999) Electromyographic activity, H-reflex modulation and corticospinal input to forearm motoneurones during active and passive rhythmic movements. Hum Mov Sci 18:307–343 Available at: http://apps.isiknowledge.com/InboundService.do?Func=Frame&product=WOS&action=retrieve&SrcApp=Papers&UT=000081560100011&SID=1EjG5lmH4nD4obmPcoJ&Init=Yes&SrcAuth=mekentosj&mode=FullRecord&customersID=mekentosj&DestFail=http%3A%2F%2Faccess.isiproducts.com%2F.

Chen R, Classen J, Gerloff C, Celnik P, Wassermann EM, Hallett M, Cohen LG (1997) Depression of motor cortex excitability by low-frequency transcranial magnetic stimulation. Neurology 48:1398–1403 Available at: http://www.neurology.org/cgi/content/abstract/48/5/1398.

Churchland MM, Cunningham JP, Kaufman MT, Foster JD, Nuyujukian P, Ryu SI, Shenoy K V (2012) Neural population dynamics during reaching. Nature 487:51–56 Available at: http://eutils.ncbi.nlm.nih.gov/entrez/eutils/elink.fcgi?dbfrom=pubmed&id=22722855&retmode=ref&cmd=prlinks.

Cros D, Soto O, Chiappa KH (2007) Transcranial magnetic stimulation during voluntary action: directional facilitation of outputs and relationships to force generation. 1185:103–116 Available at: http://www.sciencedirect.com/science?_ob=ArticleURL&_udi=B6SYR-4PNFV90-4&_user=789722&_rdoc=1&_fmt=&_orig=search&_sort=d&_docanchor=&view=c&_acct=C000043357&_version=1&_urlVersion=0&_userid=789722&md5=c36d208b1da07620a11567c0e8288645.

Darling WG, Wolf SL, Butler AJ (2006) Variability of motor potentials evoked by transcranial magnetic stimulation depends on muscle activation. Exp brain Res 174:376–385 Available at: http://link.springer.com/10.1007/s00221-006-0468-9.

Di Lazzaro V, Oliviero A, Pilato F, Mazzone P, Insola A, Ranieri F, Tonali PA (2003) Corticospinal volleys evoked by transcranial stimulation of the brain in conscious humans. Neurol Res

25:143–150 Available at: http://www.ncbi.nlm.nih.gov/pubmed/12635512?ordinalpos=1&itool=EntrezSystem2.PEntrez.Pubmed.Pubmed_ResultsPanel.Pubmed_DiscoveryPanel.Pubmed_Discovery_RA&linkpos=5&log$=relatedreviews&logdbfrom=pubmed.

Di Lazzaro V, Oliviero A, Profice P, Saturno E, Pilato F, Insola A, Mazzone P, Tonali P, Rothwell JC (1998) Comparison of descending volleys evoked by transcranial magnetic and electric stimulation in conscious humans. Electroencephalogr Clin Neurophysiol Suppl 109:397–401 Available at: http://www.sciencedirect.com/science?_ob=ArticleURL&_udi=B6T00-3TYG4RX-3&_user=789722&_rdoc=1&_fmt=&_orig=search&_sort=d&_docanchor=&view=c&_searchStrId=951859222&_rerunOrigin=google&_acct=C000043357&_version=1&_urlVersion=0&_userid=789722&md5=b47f5e8dac3.

Dounskaia N (2010) Control of human limb movements: The leading joint hypothesis and its practical applications. Exerc Sport Sci Rev.

Downey JE, Brane L, Gaunt RA, Tyler-Kabara EC, Boninger ML, Collinger JL (2017) Motor cortical activity changes during neuroprosthetic-controlled object interaction. Sci Rep 7:16947 Available at: http://www.nature.com/articles/s41598-017-17222-3.

Efron B, Tibshirani R (1993) An introduction to the bootstrap. Available at: http://books.google.com/books?id=gLlpIUxRntoC&printsec=frontcover.

Ellaway PH, Davey NJ, Maskill DW, Rawlinson SR, Lewis HS, Anissimova NP (1998) Variability in the amplitude of skeletal muscle responses to magnetic stimulation of the motor cortex in man. Electromyogr Clin Neurophysiol 109:104–113 Available at: http://eutils.ncbi.nlm.nih.gov/entrez/eutils/elink.fcgi?dbfrom=pubmed&id=9741800&retmode=ref&cmd=prlinks.

Evarts E V (1968) Relation of pyramidal tract activity to force exerted during voluntary movement. J Neurophysiol 31:14–27 Available at: http://eutils.ncbi.nlm.nih.gov/entrez/eutils/elink.fcgi?dbfrom=pubmed&id=4966614&retmode=ref&cmd=prlinks.

Flash T, Hogan N (1985) The coordination of arm movements: an experimentally confirmed mathematical model. J Neurosci 5:1688–1703 Available at: http://www.jneurosci.org/cgi/reprint/5/7/1688.

Fuglevand AJ, Winter DA, Patla AE (1993) Models of recruitment and rate coding organization in motor-unit pools. J Neurophysiol 70:2470–2488 Available at: http://www.physiology.org/doi/10.1152/jn.1993.70.6.2470.

Gallego JA, Perich MG, Miller LE, Solla SA (2017) Neural Manifolds for the Control of Movement. Neuron 94:978–984 Available at: http://linkinghub.elsevier.com/retrieve/pii/S0896627317304634.

Georgopoulos AP, Schwartz AB, Kettner RE (1986) Neuronal population coding of movement direction. Sci (New York, NY) 233:1416–1419 Available at: http://eutils.ncbi.nlm.nih.gov/entrez/eutils/elink.fcgi?dbfrom=pubmed&id=3749885&retmode=ref&cmd=prlinks.

Gribble PL, Ostry DJ (1999) Compensation for Interaction Torques During Single- and Multijoint Limb Movement. J Neurophysiol 82:2310–2326 Available at: http://jn.physiology.org/cgi/content/abstract/82/5/2310.

Gritsenko V, Hardesty RL, Boots MT, Yakovenko S (2016) Biomechanical Constraints Underlying Motor Primitives Derived from the Musculoskeletal Anatomy of the Human Arm. PLoS One 11:e0164050 Available at: http://dx.plos.org/10.1371/journal.pone.0164050.

Gritsenko V, Kalaska JF, Cisek P (2011) Descending corticospinal control of intersegmental dynamics. J Neurosci 31:11968–11979.

Gritsenko V, Yakovenko S, Kalaska JF (2009) Integration of predictive feedforward and sensory feedback signals for online control of visually guided movement. J Neurophysiol 102:914–930 Available at: http://jn.physiology.org/cgi/doi/10.1152/jn.91324.2008.

Groppa S, Schlaak BH, Münchau A, Werner-Petroll N, Dünnweber J, Bäumer T, van Nuenen BFL, Siebner HR (2012) The human dorsal premotor cortex facilitates the excitability of ipsilateral primary motor cortex via a short latency cortico-cortical route. Hum Brain Mapp 33:419–430.

Hannah R, Cavanagh SE, Tremblay S, Simeoni S, Rothwell JC (2018) Selective Suppression of Local Interneuron Circuits in Human Motor Cortex Contributes to Movement Preparation. J Neurosci 38:1264–1276 Available at: http://www.jneurosci.org/lookup/doi/10.1523/JNEUROSCI.2869-17.2017.

Hardesty RL, Boots MT, Yakovenko S, Gritsenko V (2019) The primary afferent activity cannot capture the dynamical features of muscle activity during reaching movements. bioRxiv Available at: http://biorxiv.org/content/early/2017/05/17/138859.

Hardesty RL, Olesh E V, Pollard BS, Ellaway PH, Gritsenko V (2016) Sensorimotor Transformation During Reaching Investigated with Transcranial Magnetic Stimulation and Biomechanical Simulations. In: Society for Neuroscience Meeting. San Diego, CA.

Harris C, Wolpert DM (1998) Signal-dependent noise determines motor planning. Nature 394:780–784.

Hogan N (1984) An organizing principle for a class of voluntary movements. J Neurosci 4:2745–2754.

Hollerbach JM, Flash T (1982) Dynamic interactions between limb segments during planar arm movement. Biol Cybern 44:67–77 Available at: http://eutils.ncbi.nlm.nih.gov/entrez/eutils/elink.fcgi?dbfrom=pubmed&id=7093370&retmode=ref&cmd=prlinks.

Kalaska JF, Scott SH, Cisek P, Sergio LE (1997) Cortical control of reaching movements. Curr Opin Neurobiol 7:849–859 Available at: http://www.ncbi.nlm.nih.gov/sites/entrez?cmd=Retrieve&db=PubMed&dopt=Citation&list_uids=9464979.

Kaneko K, Kawai S, Fuchigami Y, Morita H, Ofuji A (1996) The effect of current direction induced by transcranial magnetic stimulation on the corticospinal excitability in human brain. Electroencephalogr Clin Neurophysiol Suppl 101:478–482 Available at: http://www.sciencedirect.com/science?_ob=ArticleURL&_udi=B6T00-45CN0V3-2&_user=789722&_rdoc=1&_fmt=&_orig=search&_sort=d&_docanchor=&view=c&_searchStrId=952950541&_rerunOrigin=google&_acct=C000043357&_version=1&_urlVersion=0&_userid=789722&md5=3eab44075bd.

Lawrence DG, Kuypers HG (1968) The functional organization of the motor system in the monkey. I. The effects of bilateral pyramidal lesions. Brain 91:1–14 Available at:

http://eutils.ncbi.nlm.nih.gov/entrez/eutils/elink.fcgi?dbfrom=pubmed&id=4966862&retmode=ref&cmd=prlinks.

Lewis GN, Signal N, Taylor D (2014) Reliability of lower limb motor evoked potentials in stroke and healthy populations: How many responses are needed? Clin Neurophysiol 125:748–754 Available at: http://dx.doi.org/10.1016/j.clinph.2013.07.029.

MacKinnon CD, Rothwell JC (2000) Time-varying changes in corticospinal excitability accompanying the triphasic EMG pattern in humans. J Physiol 528:633–645 Available at: http://www3.interscience.wiley.com/journal/119005932/abstract?CRETRY=1&SRETRY=0.

Milner TE (2002) Adaptation to destabilizing dynamics by means of muscle cocontraction. Exp Brain Res.

Milner TE, Franklin DW (2005) Impedance control and internal model use during the initial stage of adaptation to novel dynamics in humans. J Physiol 567:651–664 Available at: http://jp.physoc.org/cgi/content/full/567/2/651.

Mizrahi J (2015) Mechanical impedance and its relations to motor control, limb dynamics, and motion biomechanics. J Med Biol Eng.

Nakamura H, Kitagawa H, Kawaguchi Y, Tsuji H (1996) Direct and indirect activation of human corticospinal neurons by transcranial magnetic and electrical stimulation. Neurosci Lett 210:45–48 Available at: http://www.sciencedirect.com/science?_ob=ArticleURL&_udi=B6T0G-3VX9DW4-D&_user=789722&_rdoc=1&_fmt=&_orig=search&_sort=d&_docanchor=&view=c&_acct=C000043357&_version=1&_urlVersion=0&_userid=789722&md5=c76f3e153e4d0251d6b3576c89ad4ae3.

Nguyen HP, Dingwell JB (2012) Proximal Versus Distal Control of Two-Joint Planar Reaching Movements in the Presence of Neuromuscular Noise. J Biomech Eng 134:061007.

Nishikawa K, Biewener AA, Aerts P, Ahn AN, Chiel HJ, Daley MA, Daniel TL, Full RJ, Hale ME, Hedrick TL, Lappin AK, Nichols TR, Quinn RD, Satterlie RA, Szymik B (2007) Neuromechanics: an integrative approach for understanding motor control. Integr Comp Biol 47:16–54 Available at: https://academic.oup.com/icb/article-lookup/doi/10.1093/icb/icm024.

Olesh E V, Pollard BS, Gritsenko V (2017) Gravitational and Dynamic Components of Muscle Torque Underlie Tonic and Phasic Muscle Activity during Goal-Directed Reaching. Front Hum Neurosci 11:1–12 Available at: https://www.frontiersin.org/article/10.3389/fnhum.2017.00474.

Penfield W, Rasmussen T (1950) The cerebral cortex of man: A Clinical Study of Localization of Function.

Prochazka A, Yakovenko S (2007) The neuromechanical tuning hypothesis. Prog Brain Res 165:255–265 Available at: http://eutils.ncbi.nlm.nih.gov/entrez/eutils/elink.fcgi?dbfrom=pubmed&id=17925251&retmode=ref&cmd=prlinks.

Rancourt D, Hogan N (2001) Stability in force-production tasks. J Mot Behav.

Robertson G, Caldwell G, Hamill J, Kamen G, Whittlesey S (2013) Research Methods in Biomechanics, 2E. Human Kinetics. Available at: http://books.google.com/books?id=gRn8AAAAQBAJ&printsec=frontcover&dq=intitle:Research+methods+in+biomechanics&hl=&cd=1&source=gbs_api.

Schieppati M, Trompetto C, Abbruzzese G (1996) Selective facilitation of responses to cortical stimulation of proximal and distal arm muscles by precision tasks in man. J Physiol 491:551–562.

Scott SH (2004) Optimal feedback control and the neural basis of volitional motor control. Nat Rev Neurosci 5:532–546.

Selen LPJ, Franklin DW, Wolpert DM (2009) Impedance control reduces instability that arises from motor noise. J Neurosci 29:12606–12616 Available at: http://eutils.ncbi.nlm.nih.gov/entrez/eutils/elink.fcgi?dbfrom=pubmed&id=19812335&retmode=ref&cmd=prlinks.

Shadmehr R, Mussa Ivaldi F (1994) Adaptive representation of dynamics during learning of a motor task. J Neurosci 14:3208–3224 Available at: http://www.jneurosci.org/cgi/content/abstract/14/5/3208.

Takahashi CD, Scheidt RA, Reinkensmeyer DJ (2001) Impedance control and internal model formation when reaching in a randomly varying dynamical environment. J Neurophysiol 86:1047–1051 Available at: http://eutils.ncbi.nlm.nih.gov/entrez/eutils/elink.fcgi?dbfrom=pubmed&id=11495973&retmode=ref&cmd=prlinks.

Talkington WJ, Pollard BS, Olesh E V, Gritsenko V (2015) Multifunctional Setup for Studying Human Motor Control Using Transcranial Magnetic Stimulation, Electromyography, Motion Capture, and Virtual Reality. J Vis Exp:e52906 Available at: http://www.jove.com/video/52906/multifunctional-setup-for-studying-human-motor-control-using.

Taylor J (2006) Stimulation at the cervicomedullary junction in human subjects. J Electromyogr Kinesiol 16:215–223.

Tazoe T, Sakamoto M, Nakajima T, Endoh T, Komiyama T (2007) Effects of remote muscle contraction on transcranial magnetic stimulation-induced motor evoked potentials and silent periods in humans. Clin Neurophysiol 118:1204–1212.

Ting LH, Chiel HJ, Trumbower RD, Allen JL, McKay JL, Hackney ME, Kesar TM (2015) Neuromechanical principles underlying movement modularity and their implications for rehabilitation. Neuron 86:38–54 Available at: http://linkinghub.elsevier.com/retrieve/pii/S0896627315001579.

Todorov E, Jordan MI (2002) Optimal feedback control as a theory of motor coordination. Nat Neurosci 5:1226–1235 Available at: http://www.nature.com/doifinder/10.1038/nn963.

Traversa R, Cicinelli P, Bassi A, Rossini PM, Bernardi G (1997) Mapping of motor cortical reorganization after stroke. A brain stimulation study with focal magnetic pulses. Stroke 28:110–117 Available at: http://eutils.ncbi.nlm.nih.gov/entrez/eutils/elink.fcgi?dbfrom=pubmed&id=8996498&retmode=ref&cmd=prlinks.

Valero-Cuevas FJ, Cohn BA, Yngvason HF, Lawrence EL (2015) Exploring the high-dimensional structure of muscle redundancy via subject-specific and generic musculoskeletal models. J Biomech 48:2887–2896 Available at: http://linkinghub.elsevier.com/retrieve/pii/S0021929015002468.

Wassermann EM, McShane LM, Hallett M, Cohen LG (1992) Noninvasive mapping of muscle

representations in human motor cortex. Electroencephalogr Clin Neurophysiol Evoked Potentials.

Winter DA (2009) Biomechanics and Motor Control of Human Movement, 4th ed. Hoboken, New Jersey: John Wiley & Sons. Available at: http://books.google.com/books?id=_bFHL08IWfwC&printsec=frontcover&dq=intitle:Biomechanics+and+motor+control+of+human+movement&hl=&cd=1&source=gbs_api.